

Supplementary Information

Ingenious construction of an electrochemical aptasensor based on an Au@COF/GO-NH₂ composite with excellent detection performance

Zhang-Ye Han,^a Hao Zhang,^b Hong-Kai Li,^a Qian-Qian Zhu,^a and Hongming He^{*a}

^a *Tianjin Key Laboratory of Structure and Performance for Functional Molecules, College of Chemistry, Tianjin Normal University, Tianjin 300387, China*

^b *Tianjin University of Technology and Education, Tianjin 300222, China*

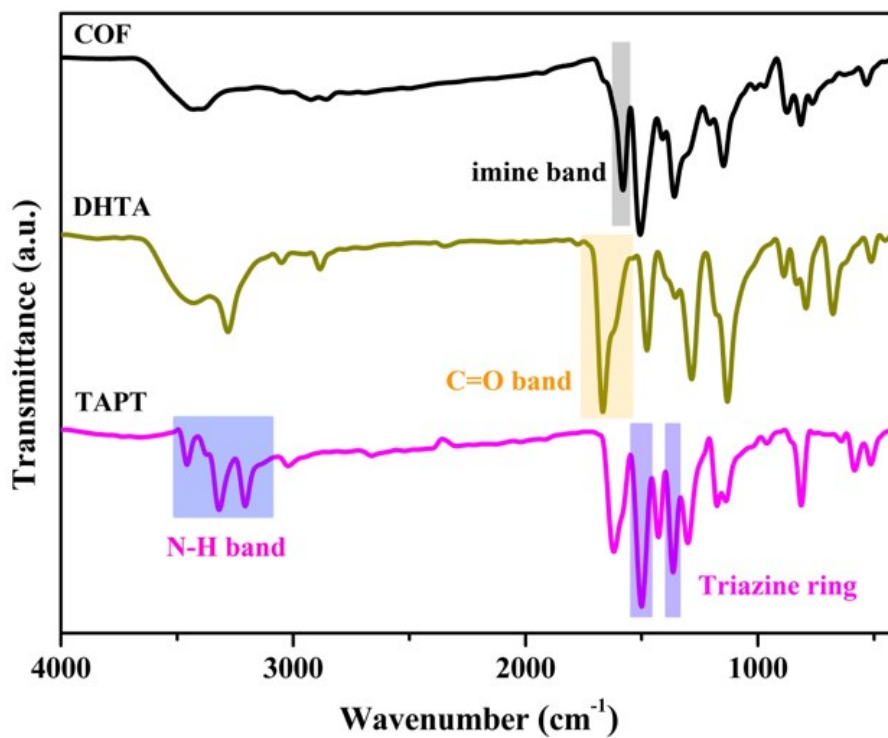


Figure S1. The FT-IR spectra of TAPT, DHTA and COF.

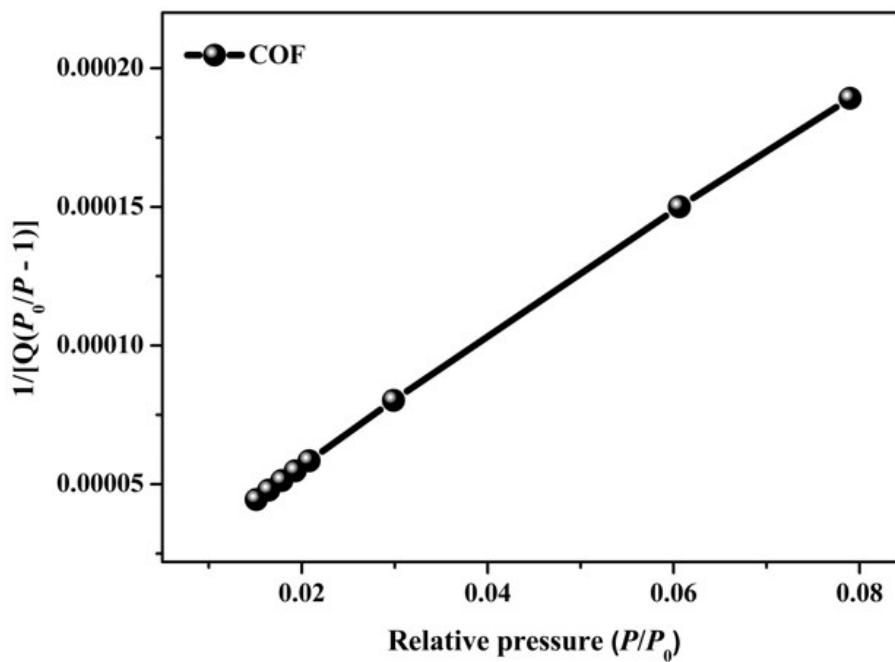


Figure S2. The BET surface area plots of COF.

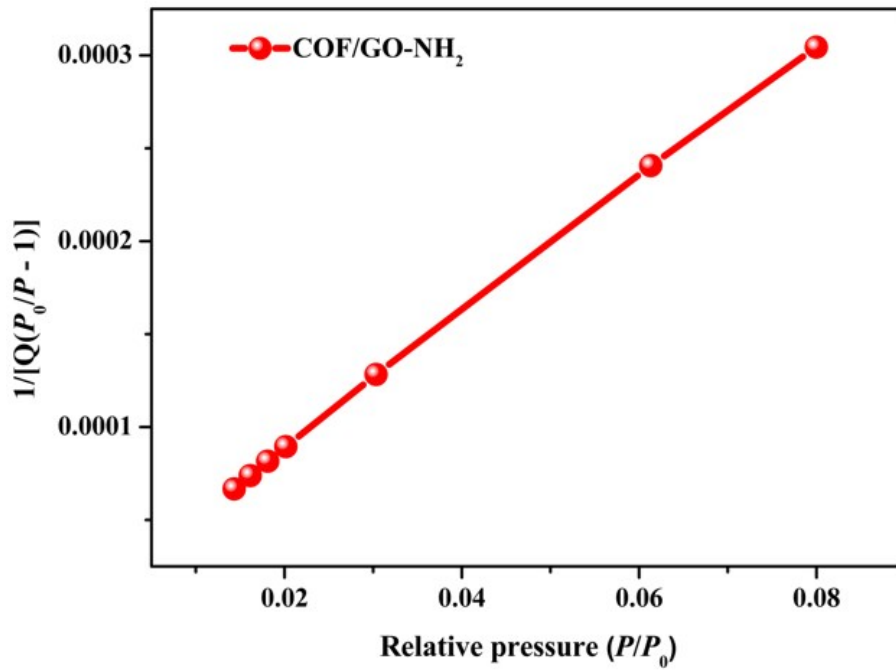


Figure S3. The BET surface area plots of COF/GO-NH₂.

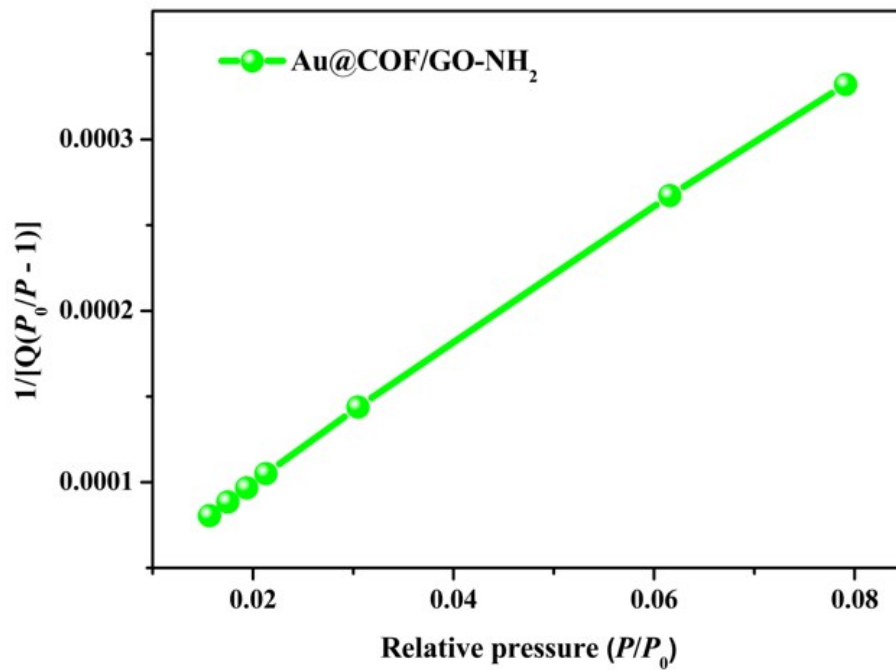


Figure S4. The BET surface area plots of Au@COF/GO-NH₂.

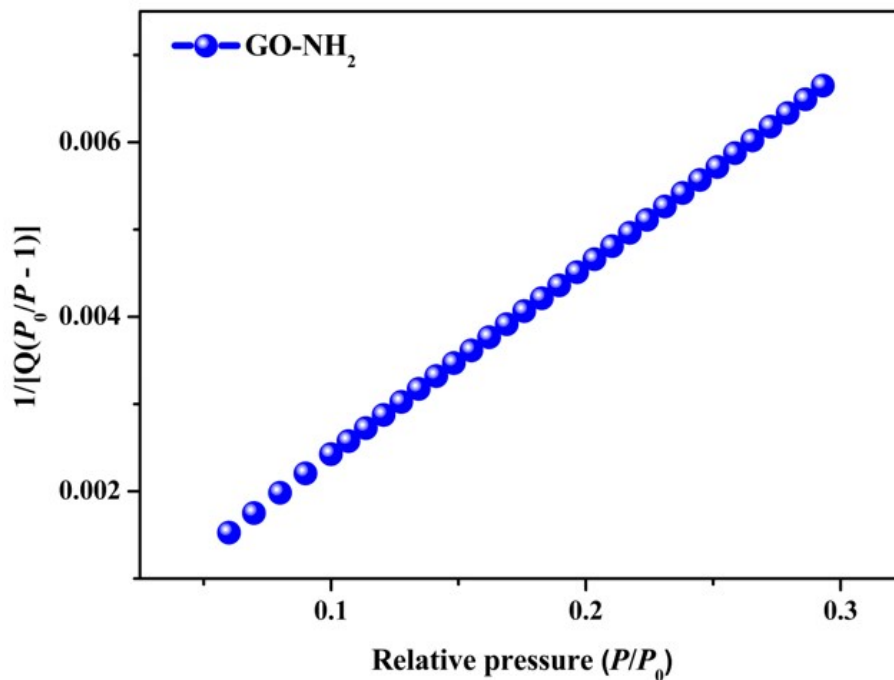


Figure S5. The BET surface area plots of GO-NH₂.

Table S1 BET surface area reports of COF, COF/GO-NH₂, Au@COF/GO-NH₂ and GO-NH₂.

Material	BET (m ² g ⁻¹)	Slope (g cm ⁻³)	Y-Intercept (g cm ⁻³)	C	Qm (cm ³ g ⁻¹)	Correlation Coefficient
COF	1907.6188 ± 13.5801	0.002271 ± 0.000016	0.000011 ± 0.000001	206.537959	438.2733	0.9998468
COF/GO-NH ₂	1193.8422 ± 8.9494	0.003630 ± 0.000027	0.000016 ± 0.000001	226.091804	274.2839	0.9998585
Au@COF/GO-NH ₂	1089.2801 ± 9.7638	0.003976 ± 0.000036	0.000020 ± 0.000002	200.119683	250.2609	0.9997975
GO-NH ₂	197.5045 ± 0.2251	0.021802 ± 0.000025	0.000236 ± 0.000005	93.408035	45.3764	0.9999802

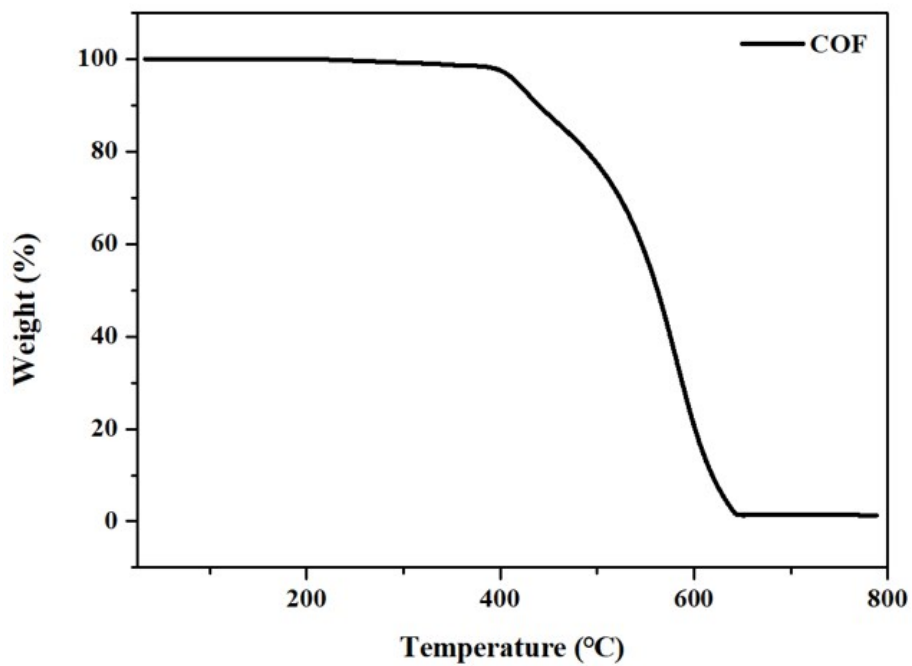


Figure S6. The TGA curve of COF.

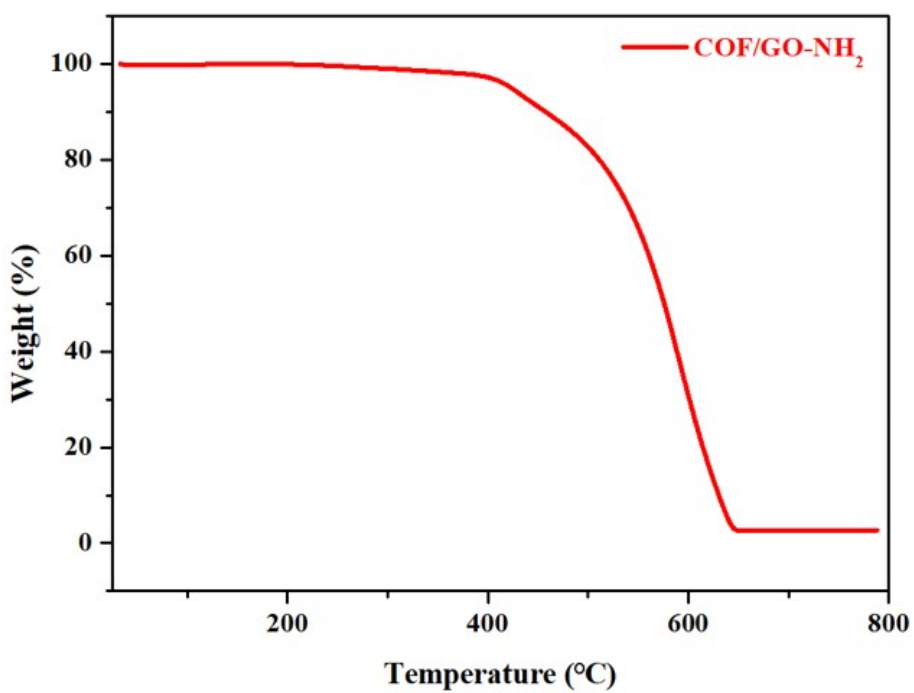


Figure S7. The TGA curve of COF/GO-NH₂.

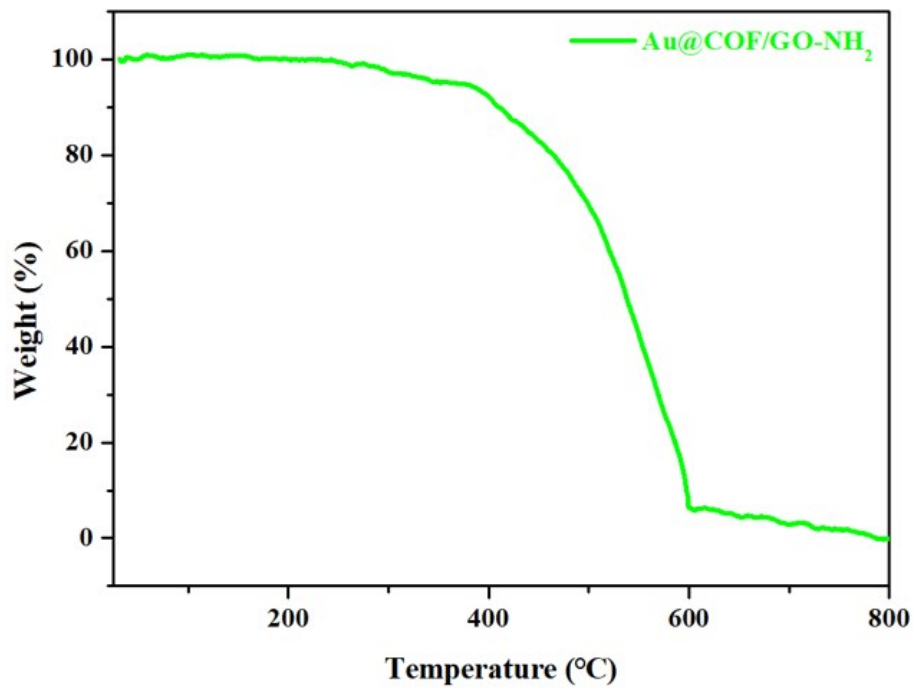


Figure S8. The TGA curve of Au@COF/GO-NH₂.

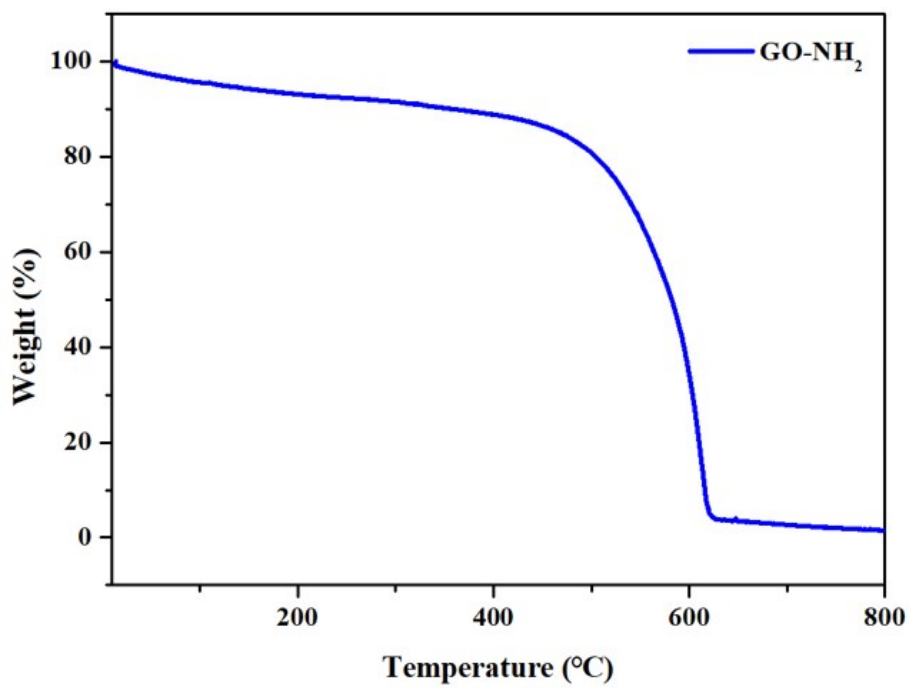


Figure S9. The TGA curve of GO-NH₂.

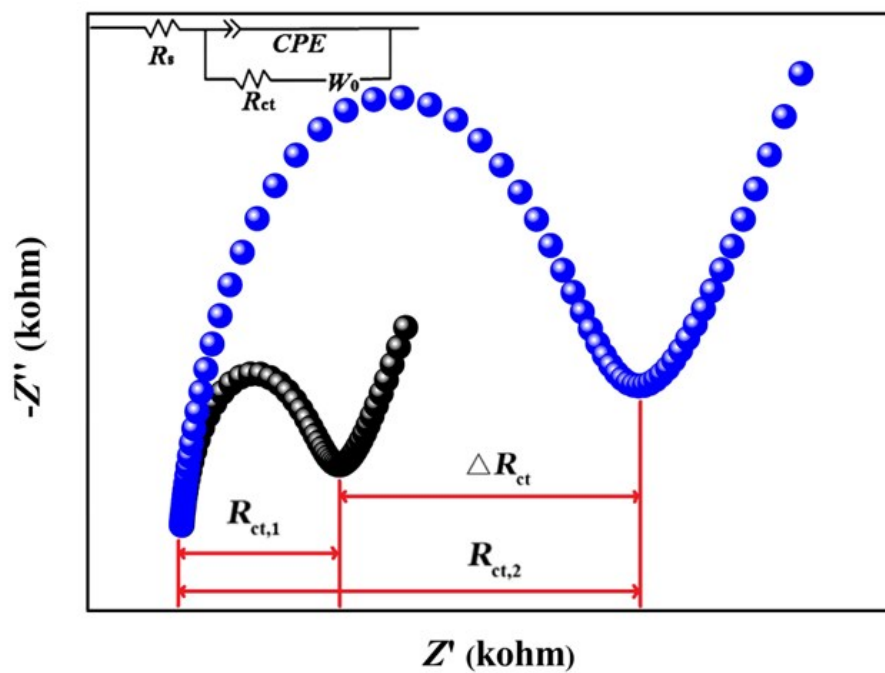


Figure S10. EIS Nyquist plots with the equivalent circuit.

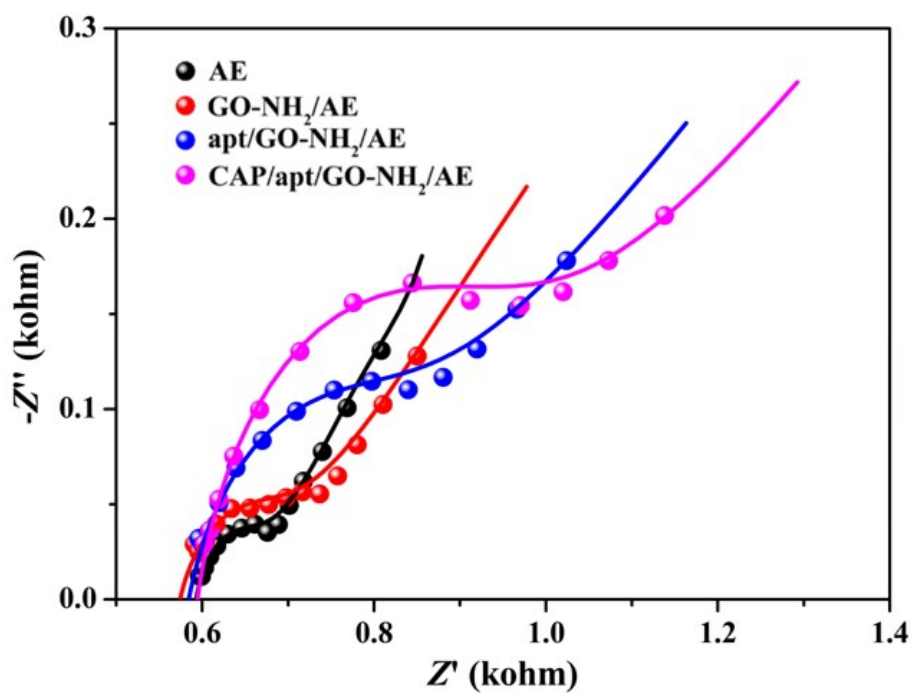


Figure S11. EIS Nyquist plots of the fabricated aptasensor based on GO-NH₂ at each stage.

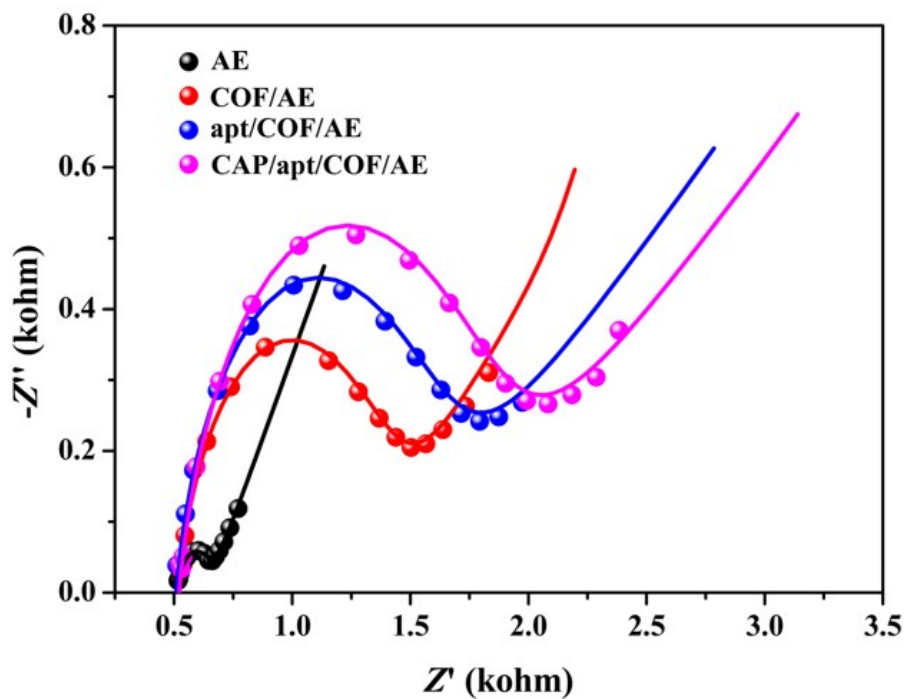


Figure S12. EIS Nyquist plots of the fabricated aptasensor based on COF at each stage.

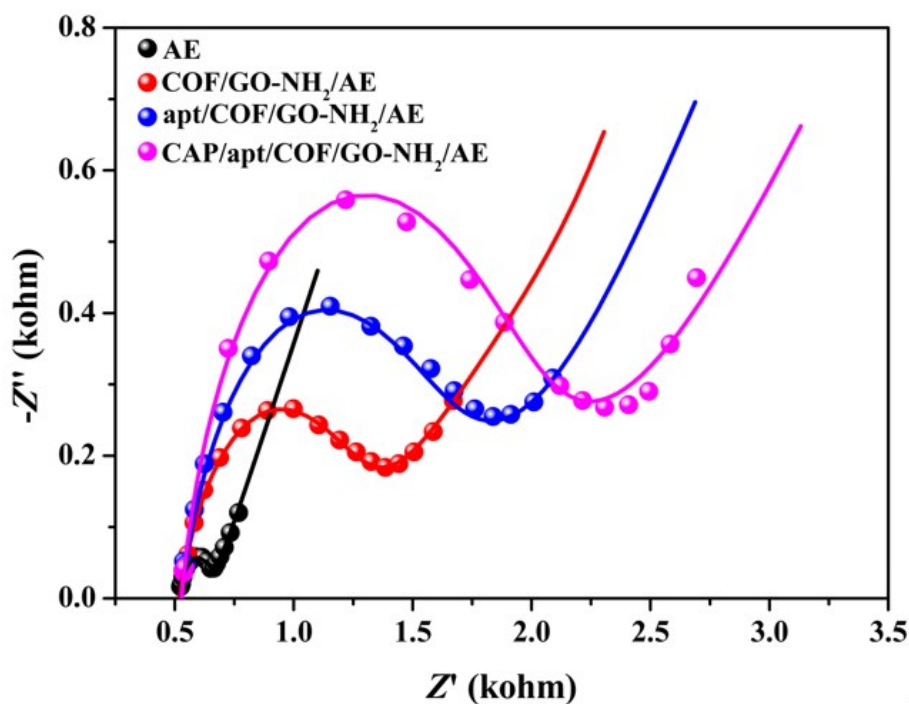


Figure S13. EIS Nyquist plots of the fabricated aptasensor based on COF/GO-NH₂ at each stage.

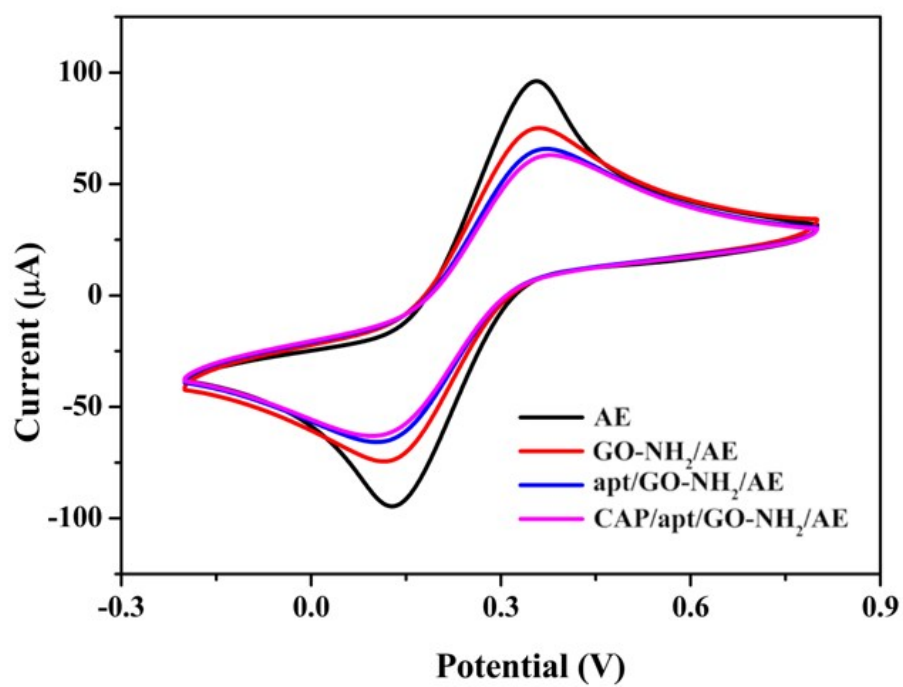


Figure S14. CV curves of the fabricated aptasensor based on GO-NH₂ at each stage.

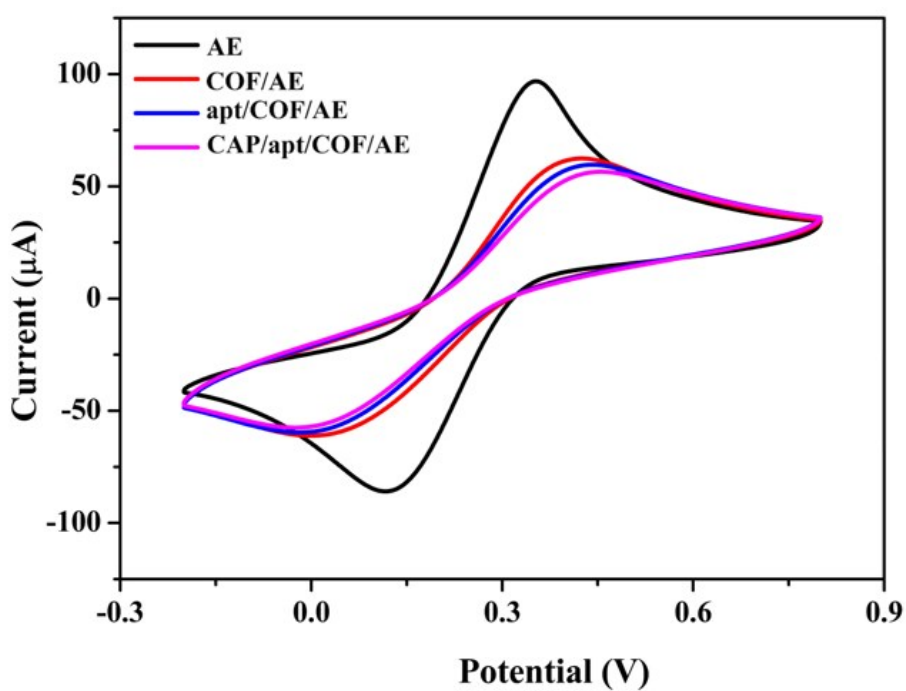


Figure S15. CV curves of the fabricated aptasensor based on COF at each stage.

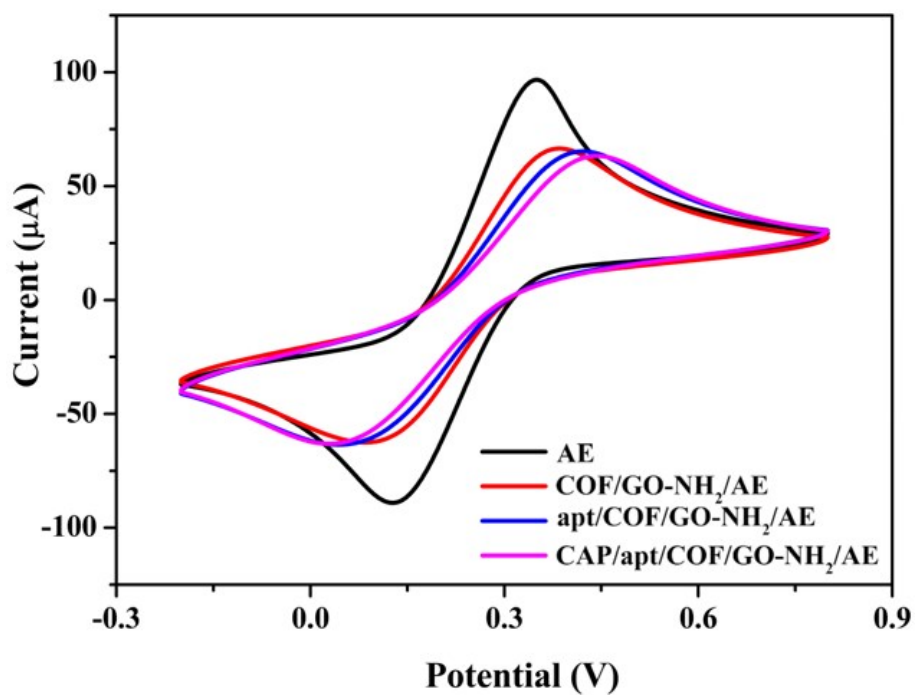


Figure S16. CV curves of the fabricated aptasensor based on COF/GO-NH₂ at each stage.

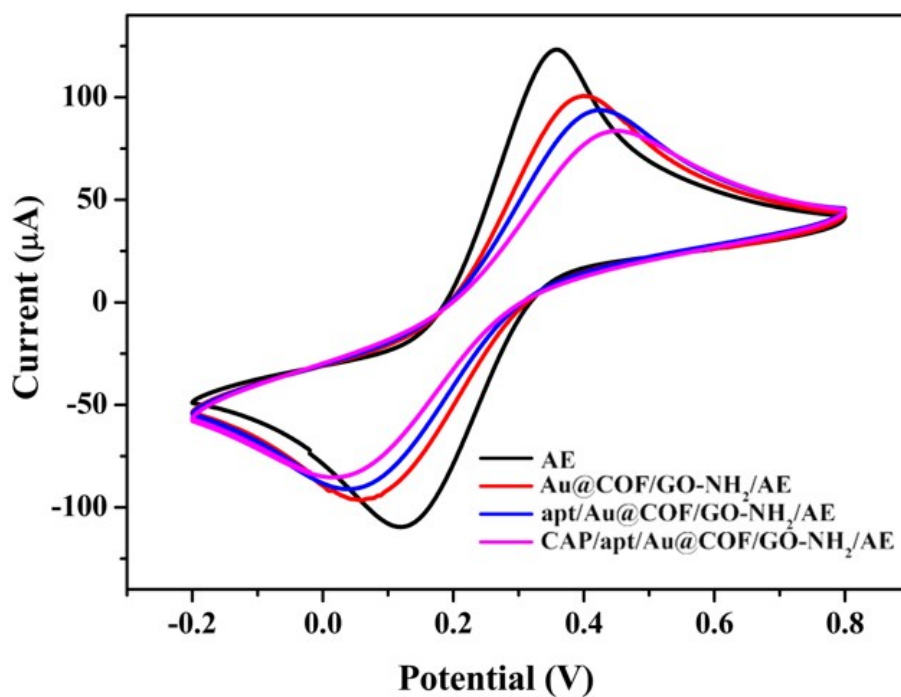


Figure S17. CV curves of the fabricated aptasensor based on Au@COF/GO-NH₂ at each stage.